BURST PRESSURE ASSESSMENT FOR PIPELINES WITH MULTIPLE CORROSION DEFECTS

Bipul Chandra, B.C. Mondal
Graduate Student, Memorial University of Newfoundland, Canada

Ashutosh Sutra Dhar
Memorial University of Newfoundland, Canada

ABSTRACT

Pipeline with multiple corrosion defects are often observed in the field. The strength of pipe with multiple corrosion patches depends on the corrosion patch intensity, their locations along longitudinal and circumferential directions of the pipe, in addition to the parameters influencing the strength of pipe with single corrosion defect. The existing design codes recommend the spacing between the corrosion patches when the interacting corrosion patches can be considered as a single patch for calculating the burst pressure of the defected pipe. In this paper, the strength and deformation characteristics of corroded pipe are investigated using finite element analysis. The parameters considered in the analysis are pipe geometries, number of corrosion patches, spacing between multiple corrosions, edge conditions (e.g. sharp and elliptical edges) and the locations of the corrosion patches. The spacing of the corrosion patches are varied along the pipe length and pipe circumference with both symmetrical and unsymmetrical orientations. The study reveals that the effect of the interaction of adjacent corrosion patches exists if the patches are located within a distance of $8t$ and $1.5\sqrt{(Dt)}$, where D is the pipe diameter and t is the pipe wall thickness. This distance is similar to the distance recommended in DNV-RP-F101 code. The distances recommended in ASME B31G and CSA Z662-15 codes appear to be un-conservative. The finite element results are compared with different burst pressure prediction models for corroded pipelines.

Keywords: Burst pressure, Corroded pipe, Multiple corrosion parches, Interaction, Stress intensity factor

1. INTRODUCTION

Pipelines are used for transporting hydrocarbons, municipal water and waste water, and for other industrial applications. The pipes often carry corrosive substance and/or are buried in corrosive environment that causes wall corrosion. The corrosion reduces the strength of the pipeline significantly and may lead to failure. A prediction of the remaining strength of corroded pipeline is required to assess the structural integrity of the pipe.

Corrosion in pipeline may occur in a single patch or in multiple patches. Researchers extensively investigated the effects of single corrosion patch on the strength of pipelines (e.g. Mondal and Dhar 2015, Chen et al. 2015a, Swankie et al. 2012, Zhou and Huang 2012, Li et al 2012, Fekete and Varga 2012). The pipe strength is generally expressed in term of the burst pressure, which is the internal pressure at the plastic collapse of the pipe. The researchers are still contributing to the improvement of the burst pressure model for determining the remaining strength of corroded pipeline. Studies on the strength of pipeline with multiple corrosion patches are also available in the literature (e.g. Dhar and Mondal 2015, Chen et al 2015b, Andrade et al. 2006, Benjamin et al. 2006, Li et al. 2011, Silva et al. 2007, Peng et al. 2011). In most of the studies, the identical sizes of corrosion patches were applied symmetrically about either a longitudinal line or a circumferential line. The effects of the spacing of the patches are however not investigated extensively. However, for multiple corrosion patches, the defects may interactively contribute to the reduction of the pipeline strength that requires additional research attention.

Design codes such as CSA Z662-15 2015, DNV RP-F101 2015, BS 7910 2013, ASME B31G 2012 codes incorporate design procedure for calculating the strength of corroded pipeline with single or multiple patches of corrosion. The

models used in the codes are however found to provide conservative and un-conservative estimations of the burst pressure (Swankie et al. 2012). Further evaluation of these design models is therefore required to calculate the burst pressure correctly.

The current paper presents a finite element (FE) investigation of the remaining strength of corroded pipe containing multiple corrosion patches. The strength of the pipe is evaluated for different orientation of the corrosion patches. The results of FE analysis are compared with those obtained using existing pipe design codes.

2. INTERACTION RULE

An interaction rule is employed to account for the interaction of multiple corrosion patches in the calculation of the burst pressure. The interaction rule states about the limiting distances along the circumferential and longitudinal directions, $(S_c)_{lim}$ and $(S_l)_{lim}$, respectively, between two successive corrosion patches beyond which the effect of interaction of the adjacent patches is negligible. Three basic types of interacting corrosion defects are generally considered, which are termed as Type 1, Type 2 and Type 3, respectively (Kiefner and Vieth 1990). In Type 1 interaction, the projections of two or more corrosion patches overlap in the longitudinal direction when projected onto a longitudinal plane passing through the wall thickness, as shown in Figure 1. The corrosion patches are separated in the circumferential direction (at distances of S_{c1}, S_{c2} …S_{cn} etc.). In Type 2, the corrosion patches are separated in longitudinal direction (at distances of S_{l1}, S_{l2}… S_{ln} etc.) as shown in Figure 2. Type 3 corresponds to a larger corroded area with localized deeper zones. The following parameters are consistently used within this paper.

D: Outer diameter of the pipe
t: wall thickness
d: maximum depth of corrosion patch
l: longitudinal extent of corrosion patch
w: circumferential extent of corrosion patch
S_l: longitudinal spacing between adjacent corrosion patches
S_c: circumferential spacing between adjacent corrosion patches

The effect of interaction of adjacent corrosion patches depends on the distance between the defects. Design codes (e.g. DNV, ASME, CSA) recommend the limiting distances (spacing), $(S_c)_{lim}$ and $(S_l)_{lim}$, in terms of different parameters. DNV code expresses the spacing in terms of pipe dimensions (diameter and thickness). ASME B31G and CSA Z662-15 codes express the spacing in terms of pipe wall thickness and the dimension of corrosion patches, respectively. Table 1 provides a summary of different recommendations for the spacing and the criteria for interaction between the patches. The effect of interaction between the defects exists when $S_l \leq (S_l)_{lim}$ or $S_c \leq (S_c)_{lim}$.

The interacting corrosions are treated as a single corrosion for calculating the burst pressure. ASME B31G (2012) code recommends using a length equals to the total length of corrosion group, l_{mn} and a depth equals to the maximum depth in the group, d_{max}. The width of the corrosion defect is not included in the ASME B31G model. DNV code (DNV-RP-F101-2015) also uses the length similar to that recommended in ASME method. The depth for corrosion group in the DNV code is calculated using Equation 1.

[1] $\quad d_{mn} = \frac{\sum_{i=m}^{i=n} d_i l_i}{l_{mn}}$

Here, d_i and l_i are the maximum depth and length, respectively, of ith corrosion of the interacting corrosion group as shown in Figure 1.

3. FE ANALYSIS

The FE analysis provides a powerful tool for modelling complex problems with non-linear material responses. Among the commercially available software for FE analysis, ABAQUS is most commonly used for analysis of pipeline. ABAQUS has the capability of modelling the non-linear deformation during yielding of corroded pipeline under high pressure. ABAQUS/Explicit module is used in this study for calculation of burst pressure of corroded pipes with multiple corrosion defects.
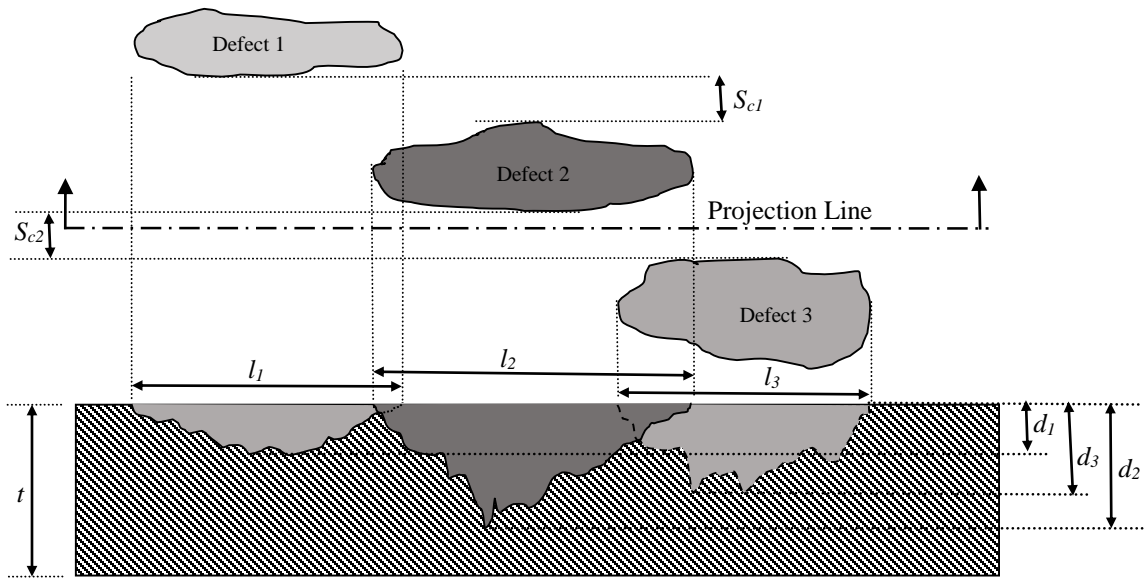
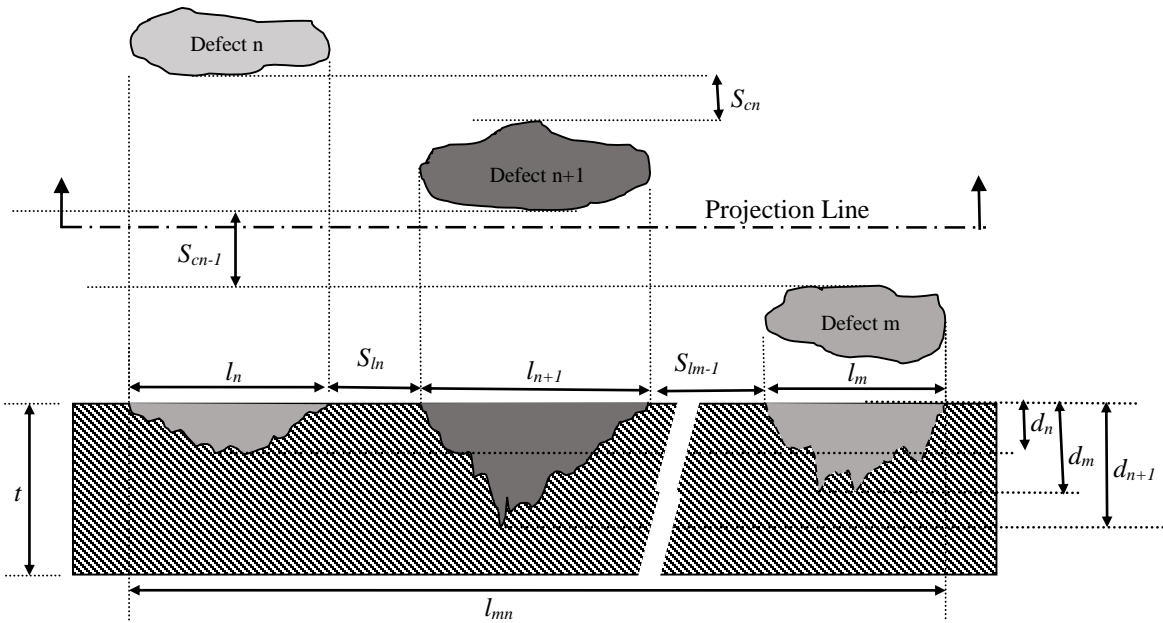Figure 1: Type 1 Interaction (DNV RP-F101 2015)

Figure 2: Type 2 Interaction (DNV RP-F101 2015)

3.1 FE Model

Although the actual geometry of corrosion patch is very complex, existing literature reveals that the failure behavior of corroded pipeline mainly depends on the maximum depth and the longitudinal extent of the corroded area. A rectangular area with constant depth (flat at the bottom) is therefore considered for idealization of the corrosion patch. The corrosion defects are created on the external surface of the pipe wall as shown in Figure 3. Sharp and smooth (curved) edges (Figure 3) are considered to investigate the effects of the edge conditions of corrosion patch on the burst pressure. An ellipse with a ratio of the major to minor axis of 2 is fitted to produce the curved edge.
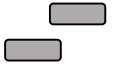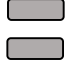
To investigate the interaction of different corrosion patches, 35 numbers of 3D Finite Element Models are developed and analyzed using ABAQUS/Explicit module. The spacing between the patches is varied independently along the longitudinal, circumferential and oblique directions. The depth of corrosion as 50% of the wall thickness is considered. The dimensions of the corrosion defects and the pipes considered in FE analysis are summarized in Table 2.

Table 1: Interaction Rule

Source	Longitudinal limit, $(S_l)_{lim}$	Circumferential limit, $(S_c)_{lim}$	Criteria for interaction
DNV RP-F101 (2015)	$2\sqrt{Dt}$	$360\sqrt{\dfrac{t}{D}}$ $(degree)$	$S_l \leq (S_l)_{lim}$ $S_c \leq (S_c)_{lim}$
ASME B31G (2012)	$3t$	$3t$	$S_l \leq (S_l)_{lim}$ $S_c \leq (S_c)_{lim}$
CSA Z662-15 (2015)	$Minimum(l_m\ to\ l_n)$	$Minimum(l_m\ to\ l_n)$	$S_l \leq (S_l)_{lim}$ $S_c \leq (S_c)_{lim}$
Kiefner and Vieth (1990)	$Minimum(6t, l_m\ to\ l_n)$	$Minimum(6t, w_m\ to\ w_n)$	$S_l \leq (S_l)_{lim}$ $S_c \leq (S_c)_{lim}$
Pipeline Operator Forum (2005)	$25.4\ mm$ (1 inch)	$6t$	$S_l \leq (S_l)_{lim}$ $S_c \leq (S_c)_{lim}$

The efficiency of FE analysis could be achieved by applying simplified boundary condition (such as symmetric condition) to the model. It is however difficult to apply simplified boundary condition to the pipes containing unsymmetric corrosion patches such as Model D and E in Table 2. For this reason, fully restraint boundary conditions at the end of the pipes are applied. To avoid the effect of boundary conditions within the corroded zone, the length of the pipes is chosen to be sufficiently long (longer than minimum length as determined by Fekete and Varge 2012).

Table 2: Pipes dimensions and corrosion geometries

Model ID	Corrosion arrangement	D (mm)	t (mm)	d/t	l (mm)	w (degree)	S_l (times t)	S_c (times t)
A	Un-corroded	300	10	-	-	-	-	-
B		300	10	0.50	60	20	-	-
C		300	10	0.50	60	20	0-10	-
D		300	10	0.50	60	20	0-10	0-10
E		300	10	0.50	60	20	3 (overlap)	0-10
F	Un-corroded	500	15	-	-	-	-	-
G		500	15	0.50	60	20	-	-
H		500	15	0.50	60	20	0-10	-
I		500	15	0.50	60	20	-	0-6

A mesh sensitivity analysis was performed to determine the optimum mesh size. Fine mesh is applied within and around the corroded area where stress concentration is expected. Coarse mesh is applied where uniform stress is expected. Appropriate gradient between coarse and fine mesh is also considered. A typical finite element mesh used in this study is shown in Figure 4.

The pipe domain is modelled using eight-node continuum element (ABAQUS element "C3D8R"). The bilinear elastic material is considered. The material properties used in the analysis are shown in Table 3. The von Mises failure criterion is used for the pipe material. The failure is thus assumed when the minimum equivalent von Mises stress on the pipe wall reaches or exceeds the ultimate tensile strength of the pipe material. Automatic time increment is chosen for the solution process in ABAQUS. The pipes under the loading of internal pressure are only considered.
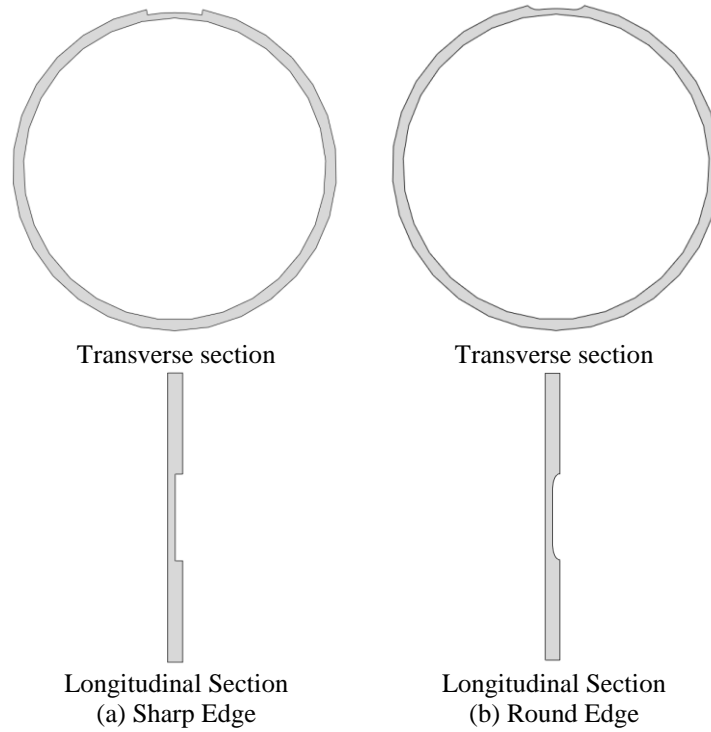

Transverse section   Transverse section

Longitudinal Section   Longitudinal Section
(a) Sharp Edge   (b) Round Edge
Figure 3: Edge condition of corrosion patch

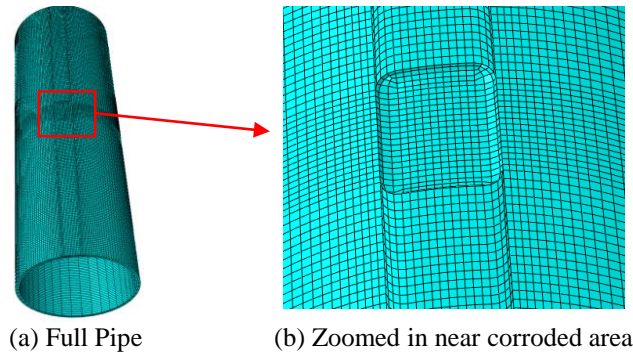(a) Full Pipe   (b) Zoomed in near corroded area
Figure 4: A typical finite element mesh

3.2 Validation of FE Model

Adequate test results on the burst pressures of corroded pipes are not available in the literature for validation of FE models for different pipe dimensions and corrosion geometries. To this end, FE models for un-corroded pipes are first validated through comparison with the results from thin-wall pressure vessel theory. Corrosions are then applied to the pipes in the validated FE models. The burst pressures for un-corroded pipes, calculated using FE analysis, are 35.91 MPa and 40.01 MPa for 300 mm and 500 mm diameter pipes, respectively. These bust pressures are comparable to those obtained using the thin-walled pressure vessel theory (within 3.25% for 300 mm diameter pipe and within 3.65% for 500mm diameter pipe). The thin-walled pressure vessel theory assumes uniform stress distribution within in the wall of the pipe, which may affect the burst pressure calculated using this theory.

Table 3: Material Properties

Property	Value
Density, ρ (kG/m^3)	7080
Young's Modulus, E (GPa)	210
Poisson's Ratio, v	0.30
Yield Strength, σ_Y (MPa)	452
Ultimate Strength, σ_U (MPa)	542
Total strain at failure, ε_U	0.043

4. RESULTS AND DISCUSSION

4.1 Edge condition of corrosion patch

Table 4 shows the burst pressures calculated considering smooth (elliptical) and sharp edges of the corrosion patches. The last column of the table shows the percent difference of the burst pressure calculated using the two models (sharp edge and smooth edge). It reveals that the difference of the burst pressure is insignificant for using the smooth edge and the sharp edge. However, the development of models and the analysis considering the smooth edge of the corrosion defects are complicated and time consuming compared to those of pipe modelled using sharp edge. Sharp edge condition is therefore considered for the rest of the analysis.

Table 4: Burst pressure for different edge conditions

D (mm)	t (mm)	d/t	l (mm)	w (degree)	Edge condition	Burst pressure (MPa)	Variation (%)
300	10	0.50	60	20	Elliptical	33.07	0.60
300	10	0.50	60	20	Sharp	32.87	
300	10	0.50	120	20	Elliptical	27.27	0
300	10	0.50	120	20	Sharp	27.27	
500	15	0.50	60	20	Elliptical	31.91	1.10
500	15	0.50	60	20	Sharp	31.56	
500	15	0.50	120	20	Elliptical	27.89	1.90
500	15	0.50	120	20	Sharp	27.36	

4.2 Interaction of corrosion patches

Figure 5 plots the burst pressure of the corroded pipe against the spacing between successive corrosion patches. The burst pressure of the corroded pipe (P) is normalized with the bust pressures of a un-corroded pipe (P_0) and plotted in the figure. The spacing are normalized using the pipe wall thickness and a dimensional parameter, $\sqrt{Dt}$, as shown in Figure 5 (a) and 5 (b), respectively. In Figure 5, the burst pressure of the corroded pipe increases with the increase of the spacing between the patches. At a spacing of 8t and 1.5$\sqrt{(Dt)}$, the increase of burst pressure is stabilized. It can thus be concluded that for the corrosion length (i.e., 60 mm) and the pipe conditions considered, the effect of interaction of the adjacent corrosion defects is minimized if the defects are spaced at a distance of 8t (and 1.5$\sqrt{(Dt)}$) or greater. This spacing is similar to the limiting spacing $(S_l)_{lim}$ recommended in DNV code (i.e. 2$\sqrt{Dt}$), indicating the DNV recommendation to be applicable for the investigated pipes. However, the values recommended in the other codes in Table 1 are un-conservative (the recommended spacing is less) with respect to the value obtained from this study.

The location of the corrosion patches appears to influence the effect of interacting corrosion defects on the burst pressure. Models C, D and E provide different burst pressures for the same pipe (300 mm diameter), as seen in Figure 5. Here, Model C corresponds to a pipe with corrosion patches on a same longitudinal line where the spacing between the patches is increased in the longitudinal direction ($S_c = 0$, $S_l = 0$ to 10t where t is the wall thickness). Model D corresponds to a pipe where the spacing (between the corrosion patches) in the longitudinal is equal to the spacing in the circumferential directions ($S_c = S_l = 0$ to 10t). Model E corresponds to a pipe with a constant spacing (between the corrosion patches) in the longitudinal direction while the spacing is varied in the circumferential direction ($S_l=3t$ (overlap), $S_c = 0$ to 10t).
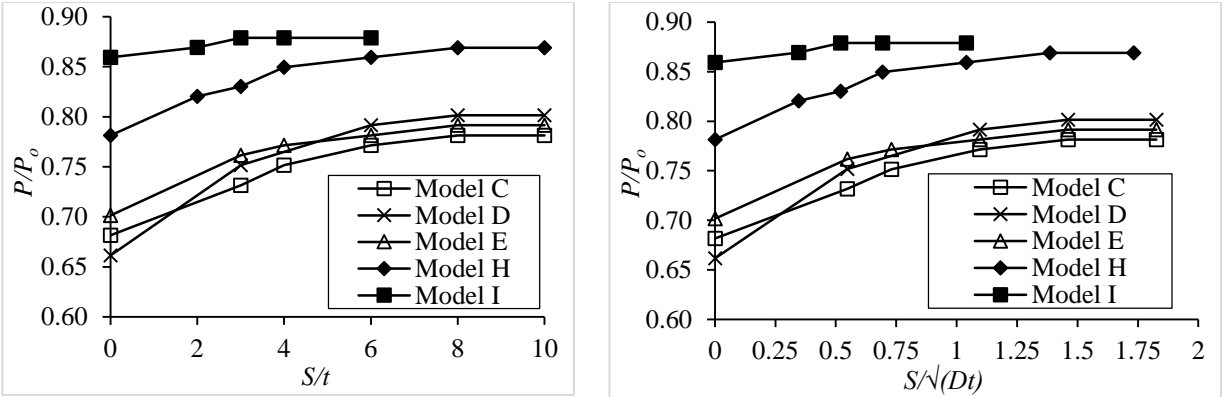
(a) Corrosion Spacing in terms of pipe wall thickness (b) Corrosion Spacing in terms of pipe dimensions

Figure 5: Effect of interaction of corrosion patches

Similar results are obtained for 500 mm diameter pipe. Model H corresponds to a pipe with corrosion patches on a same longitudinal line where the spacing between the patches is increased in the longitudinal direction ($S_c = 0$, $S_l = 0$ to $10t$). The normalized burst pressure for Model C and Model H are almost parallel, reaching the maximum value at a distance of 8t and $1.5\sqrt{(Dt)}$.

For the pipe with the corrosion patches spaced in the circumferential direction (Model I in Figure 5), the variation of the burst pressure with the spacing of the defects is less. This is due to the fact that the effect of circumferential extent of the corrosion on the burst pressure is not significant.

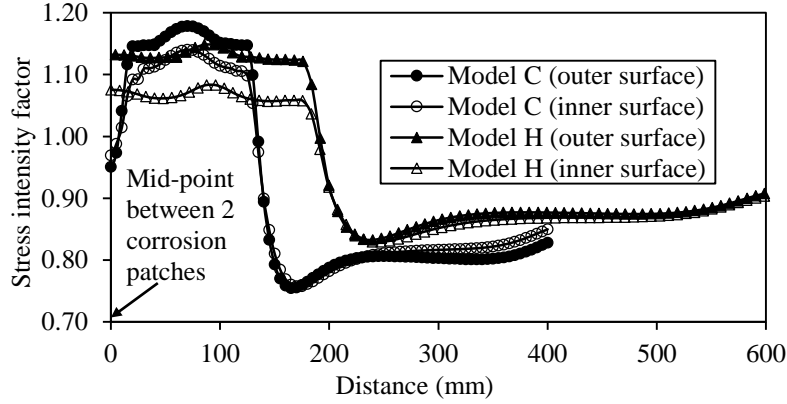**4.3 Stress and Deformation**

This section investigates the influence of interacting corrosion patches on the stress in the pipe wall. The stress is expressed in terms of stress intensity factor (SIF), which is defined as the ratio of stress in the corroded pipe to that of an un-corroded pipe subjected to the same internal pressure. Figure 6 (a) represents the SIF along the longitudinal direction of pipe passing through the centre of corrosion patches. The pipes contained two identical corrosions spaced at a distance of 8t with each other. The SIFs have been calculated at the outer surface and inner surface of pipes under the internal pressure of 25.27 MPa.

Figure 6 (a) indicates that the von Mises stress is increased significantly within the corroded zone. The stress between the corroded zones is also increased. For larger diameter pipe (Model H), the stress within the corroded zone and between the corroded zones (un-corroded area) is almost the same. This indicates that the effect of interaction between the corrosion patches exists for the large diameter pipe.

Figure 6 (b) shows the pipe wall deformation along the length of the pipe along the centreline of the corrosion patches. The figure reveals that the localized outward bending is developed within the corroded zone due to internal pressure which leads to stress redistribution within that zone.

4.4 Comparison with Design Models

The results of FE analysis are compared with design models (Modified ASME, DNV RP-F101 and CSA Z662-15) for evaluation. The results of burst pressures calculated using different codes and the FE model are included in

(a) SIF along longitudinal direction of pipe
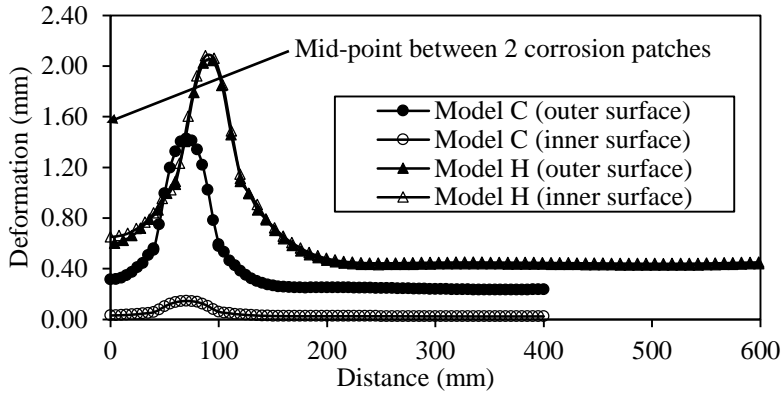
(b) Deformation along longitudinal direction of pipe

Figure 6: Stress Intensity Factor and deformation [l/t=8, P=25.27 MPa]

Table 5 along with percent deviation of design code predictions from the FE predictions. The deviations have been calculated using the Equation 2. Five corrosion configurations (Models C, D, E, H and I in Table 1) and three spacing (l/t = 3, 6 and 8) between two identical corrosion patches are considered for the comparison.

$$[2] \quad \delta = \frac{(P_{predicted} - P_{FEA})}{P_{FEA}} \times 100$$

Figure 7 plots the variation of the burst pressure calculated using three different codes with respect to the FE calculations for a 300 mm diameter pipe (Model C3 in Table 5) and a 500 mm diameter pipe (Model H3 in Table 5). The figure indicates that CSA and ASME codes are highly conservative while DNV code is less conservative in calculating the burst pressure of the corroded pipe.

5. CONCLUSIONS

This paper investigates the burst pressure of corroded pipes containing two corrosion patches located with different orientation. The following present the findings from this research:

1. FE model can be developed for corroded pipes through applying localized wall thinning. A study with a sharp and rounded edge for the corrosion patches has indicated that the effect of rounding the edges on the burst pressure of the pipeline is not significant. Corrosion patches with sharp edges can therefore be used avoiding the complexity associated with rounding the edge (smooth edge).

2. For the corrosion length (i.e., 60 mm) and the pipe conditions considered, the effect of the interaction of adjacent corrosion defects is minimized when the defects are spaced at a distance of 8t (and 1.5√(Dt)) or

greater. This distance (spacing) is similar to the value recommended in DNV code (i.e., $2\sqrt{(Dt)}$). The ASME and the CSA codes however provide a shorter distance and thus might be un-conservative.

3. The burst pressure of corroded pipe determined using different codes varies significantly from each other. Among the codes studied, the CSA and the ASME codes are found to be highly conservative while the DNV code is found to be less conservative.
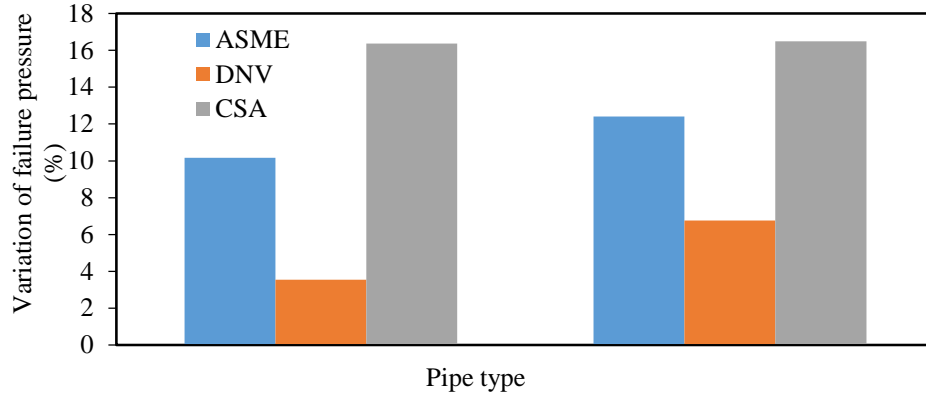

Figure 7: Deviation of burst pressure of corroded pipes [l/t=8]

Table 5: Burst pressure determined using different codes and their deviation

Model ID	l (mm)	S_l (mm)	S_c (mm)	l_{mn} (mm)	d_{mn} (mm)	P_{FEA} (MPa)	P_{ASME} (MPa)	P_{DNV} (MPa)	P_{CSA} (MPa)	Deviation, δ (%) ASME	DNV	CSA
C1	60	30	-	150	4.00	29.27	23.27	28.73	20.66	-20.50	-1.84	-29.42
C2	60	60	-	180	3.33	30.87	28.09	29.67	26.15	-9.01	-3.89	-15.29
C3	60	80	-	200	3.00	31.27	28.09	30.16	26.15	-10.17	-3.55	-16.37
D1	60	30	30	150	4.00	30.07	23.27	28.73	20.66	-22.61	-4.46	-31.29
D2	60	60	60	180	3.33	31.67	28.09	29.67	26.15	-11.30	-6.32	-17.43
D3	60	80	80	200	3.00	32.07	28.09	30.16	26.15	-12.41	-5.96	-18.46
E1	60	-30	30	90	6.67	30.47	25.76	24.51	23.43	-15.46	-19.56	-23.10
E2	60	-30	60	90	6.67	31.27	28.09	24.51	26.15	-10.17	-21.62	-16.37
E3	60	-30	80	90	6.67	31.67	28.09	24.51	26.15	-11.30	-22.61	-17.43
H1	60	45	-	165	5.45	29.81	22.46	28.43	20.27	-24.66	-4.63	-32.00
H2	60	90	-	210	4.29	30.86	27.34	28.85	26.06	-11.41	-6.51	-15.55
H3	60	120	-	240	3.75	31.21	27.34	29.10	26.06	-12.40	-6.76	-16.50
I1	60	-	45	60	-	31.56	27.34	31.42	26.06	-13.37	-0.44	-17.43
I2	60	-	90	60	-	31.56	27.34	31.42	26.06	-13.37	-0.44	-17.43
I3	60	-	120	60	-	31.56	27.34	31.42	26.06	-13.37	-0.44	-17.43

6. REFERENCES

Andrade, E.Q. d., Benjamin, A.C., Machado Jr., P.R.S., Pereira, L.C., Jacob, B.P., Carneiro, E.G., Guerreiro, J.N.C., Silva, R.C.C. and Noronha Jr., D.B. 2006. Finite element modeling of the failure behavior of pipelines containing interacting corrosion defects. *Proceedings of OMAE2006 25th International Conference on Offshore Mechanics and Arctic Engineering* Hamburg, Germany.

ASME B31G. 2012. Manual for Determining the Remaining Strength of Corroded pipelines. Supplement to the ASME B31 Code for Pressure Piping.

Benjamin, A.C., Vieira, R.D., Freire, J.L.F. and Andrade, E.Q. d. 2006. Burst tests on pipeline containing closely spaced corrosion defects. *Proceedings of OMAE2006 25th International Conference on Offshore Mechanics and Arctic Engineering* Hamburg, Germany.

BS 7910. 2013. Guide to methods for assessing the acceptability of flows in metallic structure. British Standard Institution.

Canadian Standard Association. 2015. Oil and gas pipeline systems. CSA standard Z662-15, Mississauga, Ontario, Canada.

Chen, Y., Zhang, H., Zhang, J., Li, X. and Zhou, J. 2015a. Failure analysis of high strength pipeline with single and multiple corrosions. *Journal of Materials and Design*, Elsevier, 67: 552–557.

Chen, Y., Zhang, H., Zhang, J., Liu, X., Li, X. and Zhou, J. 2015b. Failure assessment of X80 pipeline with interacting corrosion defects. *Journal of Engineering Failure Analysis*, Elsevier, 47: 67-76.

Dhar, A.S. and Mondal, B.C. 2015. FE Modelling of Corroded Pipelines under Internal Pressure. *IBC Energy 6th annual conference, Artic Oil and Gas*, North America, St. John's, Newfoundland and Labrador, Canada.

DNV-RP-F101. 2015. Corroded Pipelines. Det Norske Veritas, Norway.

Fekete, G. and Varga, L. 2012. The effect of the width to length ratios of corrosion defects on the burst pressures of transmission pipelines. *Journal of Engineering Failure Analysis*, Elsevier, 21:21-30.

Kiefner, J. F. and Vieth, P. H. 1990. Evaluating pipe Conclusion: PC program speeds new criterion for evaluating corroded pipe. *Oil & Gas Journal*, 88 (34):91-93.

Li, X., Bai, Y. and Wang, A. 2012. Study on residual strength estimation methods of corroded pipelines under internal pressure. *Proceedings of the ASME 2012 31st International Conference on Ocean, Offshore and Arctic Engineering*, OMAE2012, Rio de Janeiro, Brazil.

Li, X., Chen, Y. and Su, C. 2011. Burst capacity estimation of pipeline with colonies of interacting corrosion defects. *Proceedings of the ASME 2011 30th International Conference on Ocean, Offshore and Arctic Engineering OMAE2011*, Rotterdam, The Netherlands.

Mondal, B.C. and Dhar, A.S. 2015. Corrosion Effects on the Strength of Steel Pipes Using FEA. OMAE15, *Proceedings of the ASME 34th International Conference on Ocean, Offshore and Arctic Engineering*, St. John's, NL, Canada.

Peng, J., Zhou, C.Y., Xue, J.L., Dai, Q. and He, X.H. 2011. Safety assessment of pipes with multiple local wall thinning defects under pressure and bending moment. *Nuclear Engineering and Design*, Elsevier, 241: 2758–2765.

Pipeline Operator Forum Document. 2005. Specifications and requirements for intelligent pig inspection of pipelines, Version 3.2, January (2005).

Silva, R.C.C., Guerreiro, J.N.C. and Loula, A.F.D. 2007. A study of pipe interacting corrosion defects using the FEM and neural networks. *Advances in Engineering Software*, Elsevier, 38: 868–875.

Swankie, T., Owen, R., Bood, R., Chauhan, V., and Gilbert, G. 2012. Assessment of the remaining strength of corroded small diameter (below 6") pipelines and pipework. *Proceedings of the 2012 9th International Pipeline Conference*, IPC2012, Calgary, Alberta, Canada.

Zhou, W. and Huang, G.H. 2012. Model error assessments of burst capacity models for corroded pipelines. *International Journal of Pressure Vessels and Piping*, Elsevier, 99-100: 1-8.